RESEARCH ARTICLE doi.org/10.1002/adsc.202100491

Advanced Synthesis & Catalysis

C_1-Symmetric Atropisomeric NHC Palladium(II) Complexes: Synthesis, Resolution and Characterization

Lingyu Kong,[a] Yajie Chou,[a] Marion Jean,[a] Muriel Albalat,[a] Nicolas Vanthuyne,[a] Paola Nava,[a] Stéphane Humbel,[a] and Hervé Clavier[a,*]

[a] Aix Marseille Univ, CNRS, Centrale Marseille, iSm2, Marseille, France
Phone: +33 (0)413 945 630
E-mail: herve.clavier@univ-amu.fr

Manuscript received: April 22, 2021; Revised manuscript received: June 22, 2021;
Version of record online: July 14, 2021

Supporting information for this article is available on the WWW under https://doi.org/10.1002/adsc.202100491

Abstract: Series of chiral palladium(II) allyl and cinnamyl complexes bearing a C_1-symmetric N-heterocyclic carbenes were synthesized from achiral precursors. The chirality of theses complexes results from the formation of the carbene-palladium bond which restricts the rotation of dissymmetric *N*-aryl substituents of the NHC and thus creates an axis of chirality. Chiral HPLC at preparative scale enabled the resolution of racemic complexes and provided a straightforward access to complexes with excellent enantiopurities (>99.5% ee). Enantiopure complexes were studied by crystal X-ray diffraction and electronic circular dichroism (ECD). Their configuration stabilities were investigated both experimentally and theoretically through the determination of the rotational barrier values. These complexes were tested for the intramolecular α-arylation of amides, with a moderate chiral induction (up to 54% ee).

Keywords: axial chirality; NHC ligand; Palladium; Chiral HPLC; ECD

Introduction

Nowadays, N-heterocyclic carbenes (NHC) are well-established ancillary ligands in organometallic chemistry.[1] Their unique stereoelectronic properties allow to obtain highly reactive catalytic species and contributed to the development of a wide array of metal-catalyzed transformations.[2] Moreover, well-defined complexes bearing an NHC ligand are often particularly stable toward air and moisture. Many metal-NHC complexes can even be purified by silica gel chromatography. Therefore, the development of chiral versions has attracted much attention.[3] Several designs of chiral monodentate NHC ligands have been investigated, such as the use of chiral *N*-substituents (**A**, Figure 1a). In spite of remarkable achievements,[4] chiral catalysts **A** generally suffer from a high flexibility of chiral *N*-substituents that can be circumvented with fused skeletons, structure **B**.[5] The main other strategy consists in the introduction of chiral centers on the NHC backbone (Figure 1b). Even if chiral centers are positioned far away from the metal center, in some case, excellent chiral induction can be reached with catalysts of structure **C**.[6] In 2001, Grubbs disclosed that the use of dissymmetric aryl groups as *N*-substituents allow for improving the enantioinduction through a relay effect (structure **D**).[7] Despite successful and widespread applications,[8] conformational insights have been thoroughly studied only in rare occasions.[9] In absence of determinations of rotational barriers of aryl groups along the C–N bonds, configurational stabilities are difficult to assess (rotamers vs. atropisomers). Axial chirality has also been implemented for the design of chiral NHC ligands (Figure 1c). Among various examples,[10] structures **E**[11] and **F**[12] are of interest, albeit often prepared through tedious and time-consuming syntheses. Recently, we disclosed a new concept of chiral metal-NHC complexes by virtue of a rotationally restricted C–N axes leading to the formation of atropisomers (Figure 1d).[13] Of note, since the systematic name for this category of NHC ligands is quite cumbersome a trivial name "IKong" has been assigned.

Advantageously, our strategy does not require the use of chiral precursors for which supplies, prices and purities might fluctuate. As the metal-NHC bond formation generates atropisomers by means of the C–N bond rotation restriction, chiral HPLC separation

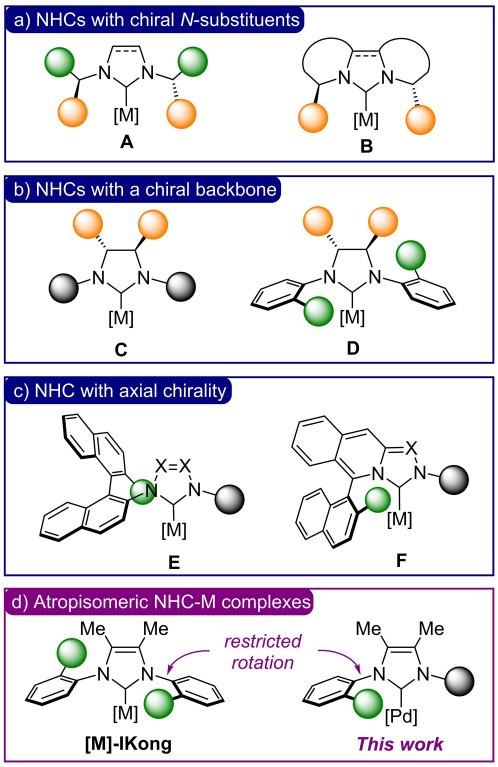

Figure 1. Designs of chiral monodentate NHC ligands.

at preparative scale gave an access to both enantiomers. Copper and palladium complexes bearing IKong have shown good performances in enantioselective catalysis. Herein, we disclosed the synthesis of C_1-symmetric atropisomeric NHC palladium complexes and their resolution by chiral HPLC at preparative scale to afford homochiral complexes with excellent optical purities. Taking advantage of the C_1-symmetry compared to the C_2-symmetry which requires the consideration of *meso* diastereomers, these complexes were used to determine accurately the values of the rotational barriers and thus identify the key parameters to design configurationally stable NHC-metal complexes such as the necessity of methyl groups on the NHC backbone.

Results and Discussion

Imidazolium Salts Synthesis

For the synthesis of imidazolium salts **4** containing methyl groups on the backbone, we first experienced the synthetic route disclosed by Fürstner in 2006.[14] As depicted in Scheme 1, formamide **3** was prepared in an excellent yield from 3-hydroxybutan-2-one **1** and 2-isopropylaniline giving rise to α-aminoketone **2** and subsequent formylation using acetic formic anhydride. Of note, the acid catalyzed substitution could not be achieved with the bulky 2,6-diisopropylaniline. With cyclohexylamine, the one-pot reaction including three steps allowed to isolate imidazolium salt **4b** with a satisfying yield of 49%. With the less nucleophilic 2,6-diisopropylaniline, the yield of **4e** dropped down to 15% and the purification step was found demanding. At room temperature, the ^{1}H NMR spectra of imidazolium salt **4b** displayed clearly signals of inequivalent chemical shifts due to the presence of the diastereotopic isopropyl group which suggests a slow interconversion of enantiomeric conformers on the NMR timescale. In order to quantify the rotational barrier around the C–N bond, variable temperature ^{1}H NMR experiments were carried out and showed the effect of the temperature on lineshape up to signals coalescence (Figure 2). Eyring analysis allowed to extract the kinetic parameters for the C–N bond rotation and these results were corroborated by DFT theoretical calculations (Figure 3). In order to simplify calculations, a methyl group was used as *N*-substituent instead of cyclohexyl. Of note, the results presented later demonstrate that the nature of this *N*-substituent does not play a significant role on the rotational barriers values. The experimental value of the rotational barrier of imidazolium salt **4b** (82 kJ.mol^{-1}; i.e. $t_{1/2}$ = 13 s at 25 °C) is in good agreement with the lowest calculated value (**4a**, 87.3 kJ.mol^{-1}). The DFT approach allowed us to confirm that the rotation takes place on the hydrogen side as demanding on the backbone side ($\Delta G^{\neq}_{(BB)}$ = 128 kJ.mol^{-1}). Calculations performed on the carbene **5a** showed that the rotation is by 20 kJ.mol^{-1} easier on the carbene side compared to the hydrogen side for imidazolium **4a**. This magnitude difference is in line with literature results.[9b] More surprisingly, the rotation on the backbone side

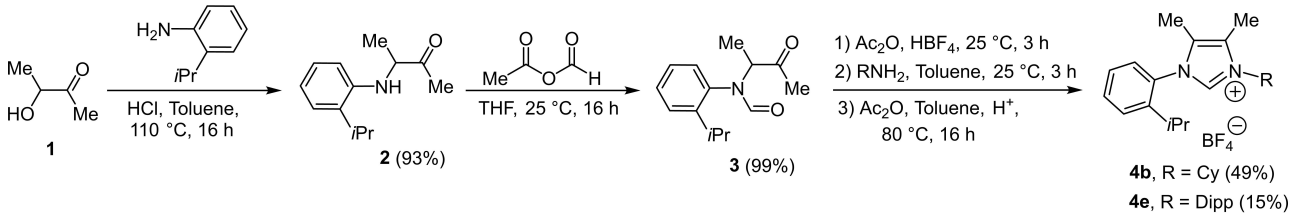

Scheme 1. Preparation of imidazolium salt **4** according to Fürstner's method. (Dipp = 2,6-diisopropylphenyl).

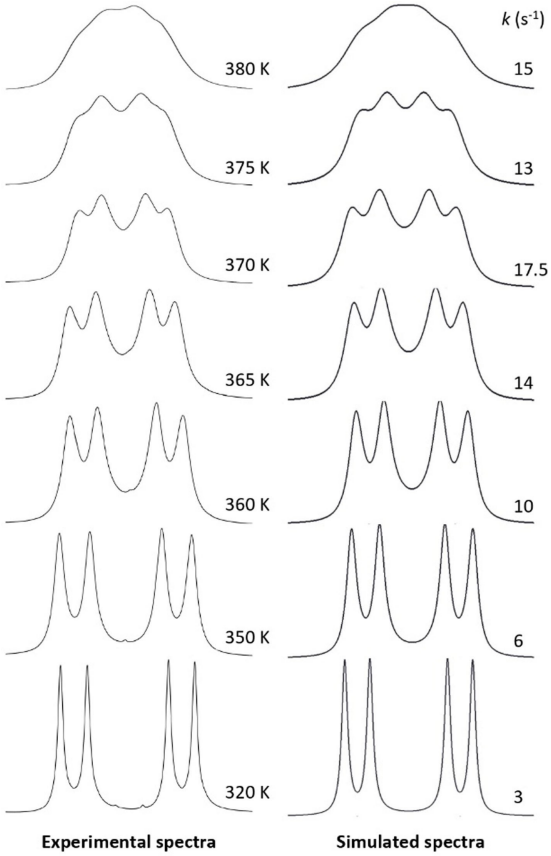

Figure 2. Variable temperature ^{1}H NMR spectra of imidazolium salt **4b** in $C_2D_2Cl_4$ and the corresponding lineshape simulations.

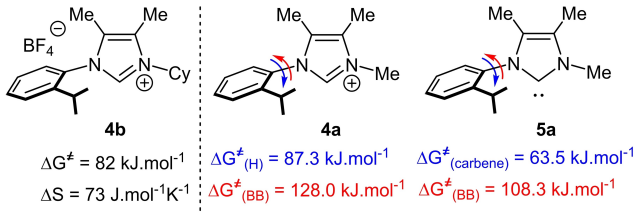

Figure 3. Values for the rotational barriers of imidazolium salts **4a** and **4b** and the corresponding free carbene **5a** (left: experimentally determined; right DFT calculated).

was found also by 20 kJ.mol^{-1} easier for the carbene form compared to the imidazolium ($\Delta G^{\neq}_{(BB)}$ = 108.3 kJ.mol^{-1} vs. 128 kJ.mol^{-1}).

As the synthetic procedure developed by Fürstner was found not convenient for the synthesis of imidazolium salt with methyl substituents on the backbone, we then tested the methodology reported by Glorius (Scheme 2).[15] Dissymmetric formamidines **6** were prepared in low to moderate yields from 2-isopropylaniline and triethylorthoformate and subsequent addition of amine. Then, formamidines **6** reacted with 3-bromo- butanone in presence of diisopropylethylamine in acetonitrile at 110 °C for 20 h to give rise to the cyclized products **7** which were not isolated and treated with acetic anhydride and HBF_4 in toluene at 80 °C for 16 h. Imidazolium salts **4b–d** were obtained in low to moderate yields but products were easily purified. Unexpectedly, under the same reaction conditions, formamides containing two aromatic substituents **6e–g** did not lead to the corresponding cyclized products **7**, but alkylated products **8** were formed but not characterized due to a large number of isomeric forms (Scheme 3). From **8** to get imidazolium salts **4** we applied the procedure reported by Shi.[16] A treatment with triflic anhydride and trimethylamine gave rise to the imidazolium salts **4e′–g′** with triflate as counterion in moderate yields (from 34 to 51%).

Palladium Complexes Preparation and Resolution

With 6 imidazolium salts **4** in hands, we prepared the corresponding Pd(allyl)Cl complexes **9** by generation of the carbene with *t*BuOK in presence of the dimer $[Pd(allyl)Cl]_2$ (Scheme 4). These complexes were found very stable and therefore could be purified by silica gel chromatography to give the pure complexes in good yields. The same procedure was applied to the synthesis of Pd(cinnamyl)Cl complexes **10** which were isolated in good to quantitative yields and displayed also excellent stabilities (Scheme 5). The ^{1}H NMR spectra of complexes **9** and **10** are somewhat intricate due to the presence of at least two isomeric forms. For the same reason, ^{13}C NMR spectra show a multitude of peaks, but characteristic carbenic carbons were observable in the range 178–182 ppm.[17]

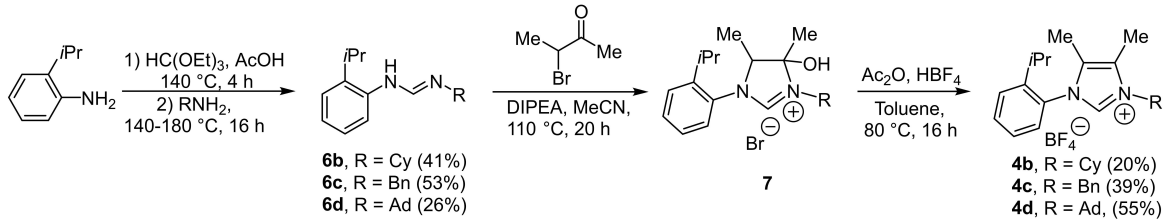

Scheme 2. Preparation of imidazolium salt **4** according to Glorius' synthetic procedure.

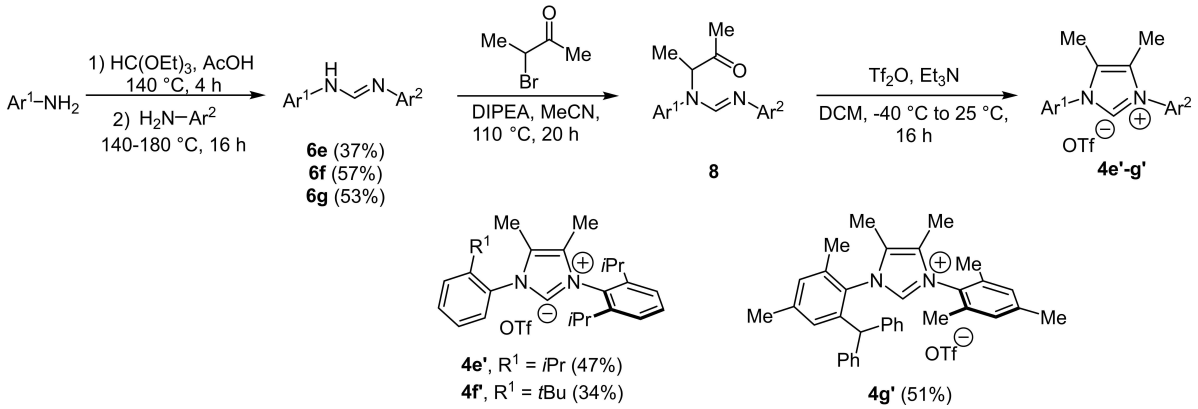

Scheme 3. Preparation of imidazolium salt **4** according to the procedure reported by Zhang and Shi.

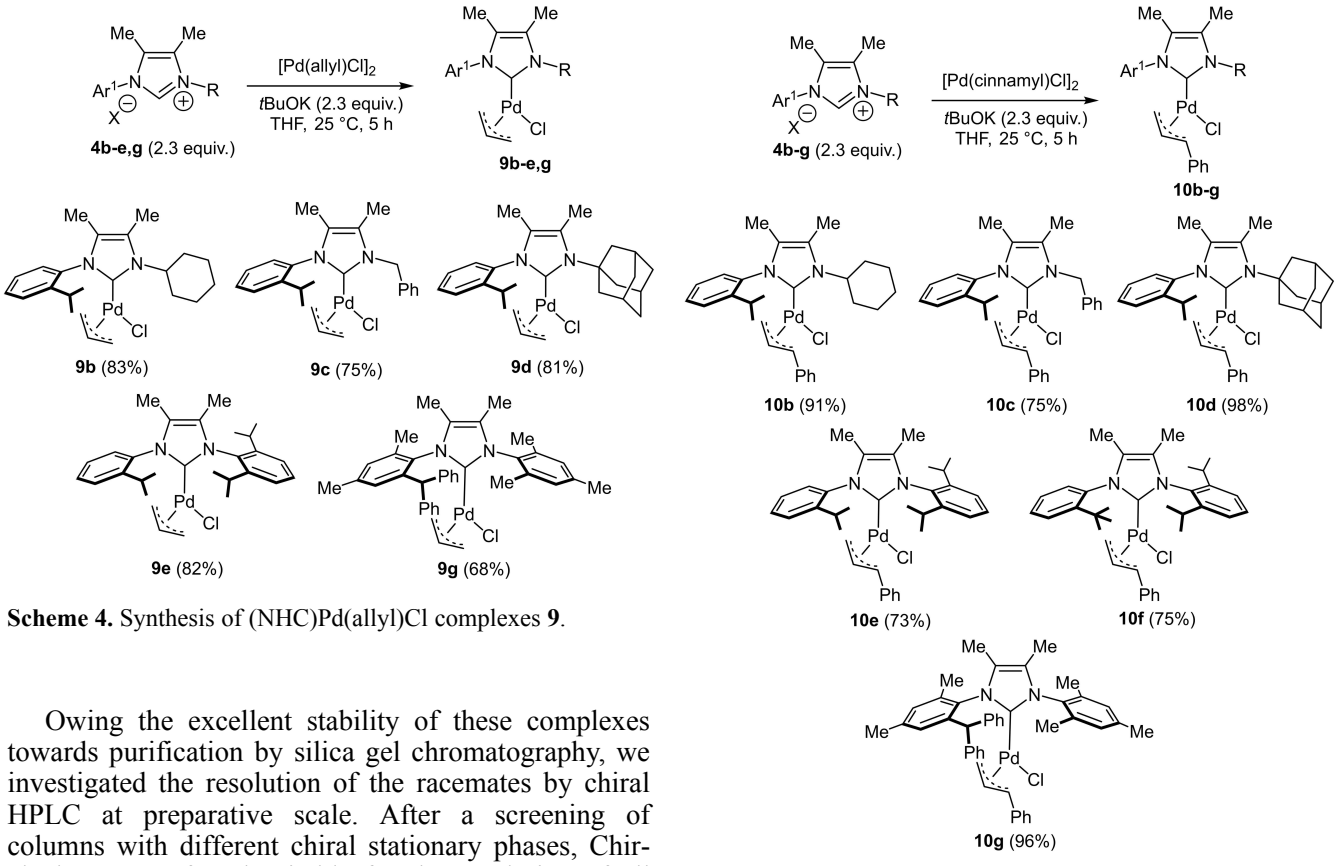

Scheme 4. Synthesis of (NHC)Pd(allyl)Cl complexes **9**.

Scheme 5. Preparation of (NHC)Pd(allyl)Cl complexes **10**.

Owing the excellent stability of these complexes towards purification by silica gel chromatography, we investigated the resolution of the racemates by chiral HPLC at preparative scale. After a screening of columns with different chiral stationary phases, Chiralpak IG was found suitable for the resolution of all complexes. With a 1 cm diameter column, batches from 50 to 250 mg could be purified in few hours. Selected details are gathered in Table 1.[17] Both enantiomers of each palladium complexes were isolated in good to excellent yields (34–49%; 71–95% overall yields) and remarkable enantiopurities, in most of the case >99.5% ee. Moreover, no racemization process was observed during the resolution suggesting a good configurational stability of the palladium complexes. The examination of specific rotations revealed that the direction of plane-polarized light rotations does not change between allyl- and cinnamyl-containing complexes. For example, the first eluted enantiomer of **9b** is dextrorotary as well as the first eluted complex **10b** (entries 1 and 6). The only exception is for complexes containing an adamantyl *N*-substituent, complexes **9d** and **10d**, for which the first eluted enantiomer **9d** is levorotary whereas dextrorotary for **10d** (entries 3 and 8). It seems that the first eluted enantiomers of complexes bearing an alkyl *N*-substituent rotate plane-polarized light clockwise (en-

Table 1. Resolution by chiral HPLC of heterochiral complexes **9** and **10**.

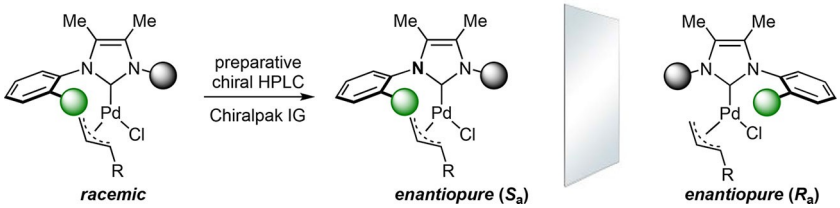

Entry	Complex (Racemate quantity)	Complex	1st eluted Quantity	Yield	ee (%)	Complex	2nd eluted Quantity	Yield	ee (%)	Overall yield
1	**9b** (69 mg)	(S_a)-(+)-**9b**[a]	34 mg	49%	>99.5	(R_a)-(−)-**9b**[a]	32 mg	46%	>99.5	95%
2	**9c** (132 mg)	(S_a)-(+)-**9c**[b]	49 mg	37%	>99.5	(R_a)-(−)-**9c**[b]	45 mg	34%	>99.5	71%
3	**9d** (213 mg)	(S_a)-(−)-**9d**[a]	94 mg	44%	>99.5	(R_a)-(+)-**9d**[b]	95 mg	45%	>99.5	89%
4	**9e** (51 mg)	(S_a)-(−)-**9e**[b]	22 mg	43%	>99.5	(R_a)-(−)-**9e**[b]	24 mg	47%	>99.5	90%
5	**9g** (170 mg)	(S_a)-(−)-**9g**[b]	70 mg	41%	>99.5	(R_a)-(−)-**9g**[b]	68 mg	40%	>99.5	81%
6	**10b** (106 mg)	(S_a)-(+)-**10b**[a]	45 mg	43%	>98.5	(R_a)-(−)-**10b**[a]	43 mg	41%	>98.5	84%
7	**10c** (110 mg)	(S_a)-(+)-**10c**[a]	40 mg	36%	>99.5	(R_a)-(−)-**10c**[a]	42 mg	38%	>99.5	74%
8	**10d** (105 mg)	(R_a)-(+)-**10d**[a]	39 mg	37%	>99.5	(S_a)-(−)-**10d**[a]	44 mg	42%	>99.5	79%
9	**10e** (55 mg)	(S_a)-(−)-**10e**[a]	25 mg	46%	>99	(R_a)-(+)-**10e**[a]	24 mg	44%	>99	90%
10	**10f** (135 mg)	(S_a)-(−)-**10f**[a]	53 mg	39%	>99.5	(R_a)-(+)-**10f**[a]	51 mg	38%	>99.5	77%
11	**10g** (250 mg)	(S_a)-(−)-**10g**[b]	105 mg	42%	>99.5	(R_a)-(+)-**10g**[b]	95 mg	38%	>98.5	80%

[a] Absolute configuration deduced from ECD spectra comparison.
[b] Absolute configuration determined by XRD spectroscopy.

tries 1,2 6 and 7), whereas the first eluted of complexes containing aryl *N*-substituents are levorotary (entries 4, 5 and 9–11).

Absolute Configuration Assignments

In spite of repeated attempts, suitable crystals for single crystal X-ray diffraction studies could be grown only for enantiopure 2nd eluted complexes **9c**, **9e**, **9g** and **10g**. Ball-and-stick representations depicted in Figure 4 allowed to unambiguously establish the structures, the atoms connectivity, as well as the absolute configurations thanks to Flack parameters refined to value of zero. These complexes show the expected distorted square planar geometry around the metal center. The carbene-Pd bond distances are between 2.027(3) and 2.037(5) Å, and the Pd-allyl and Pd-cinnamyl bond lengths are respectively in the ranges of 2.101(5)–2.194(8) Å and 2.102(6)–2.264(6) Å. These values are comparable to those found in similar complexes.[18]

With the single crystal X-ray diffraction data in hands, the buried volumes (%V_{Bur}), a parameter describing the bulkiness of a ligand in the first coordination sphere of a metal, and topographic steric maps have been determined (Figure 5).[19] As expected, the NHC bearing a benzyl *N*-substituent (complex **9c**) was found significantly less bulky than other NHC containing mesityl or Dipp as *N*-substituent (%V_{Bur} = 35.2% vs. 36.8–37.5%). No significant difference could be noticed either for %V_{Bur} values or steric maps,

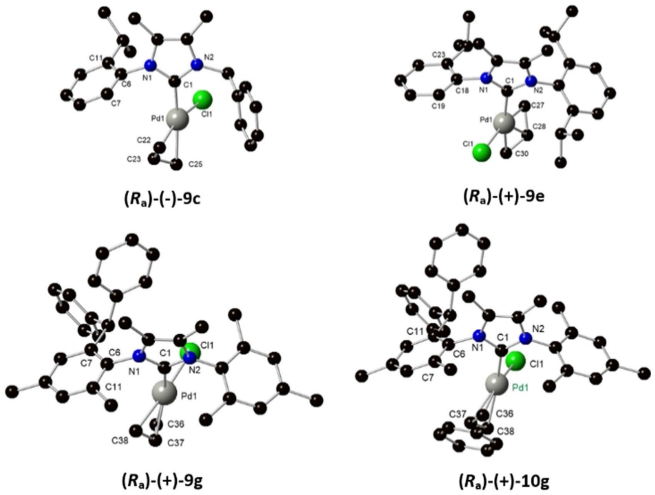

Figure 4. Ball-and-stick representations of enantiopure palladium complexes (hydrogens have been omitted for clarity).

between allyl- and cinnamyl-containing complexes **9g** and **10g**. The steric map of NHC ligand bearing complex **9c** (upper left corner) does not allow the identification of the clear zones of different steric pressures and suggests a low chiral induction in asymmetric catalysis. In contrast, the steric map of complex **9e** NHC (upper right corner) exhibits a substantial difference of steric pressure between the northeast and northwest quadrants. A more pronounced difference was observed between these quadrants for

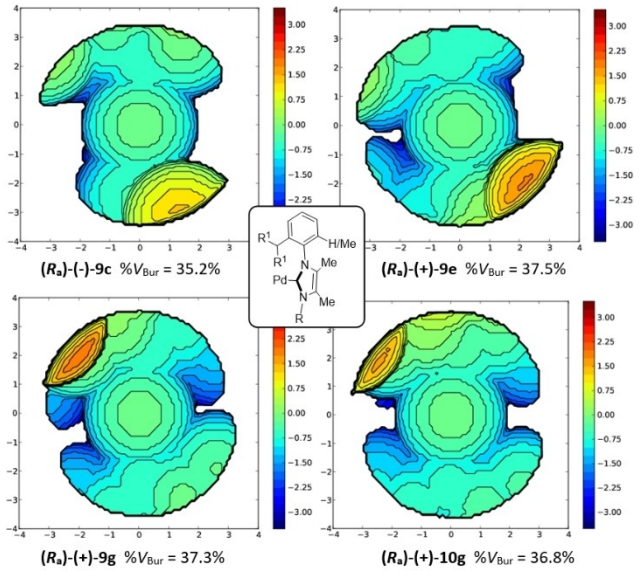

Figure 5. Steric contour maps of NHC ligands (complexes are oriented as shown in the central sketch).

the NHC ligand of complexes **9 g** and **10 g** and suggests a better ability to induce an enantioselectivity.

UV-vis and ECD spectra for both enantiomers of all the palladium complexes have been measured in acetonitrile solutions. Individual ECD spectra, reported in the supporting information, showed expected nearly mirror-images for both enantiomers. As Electronic Circular Dichroism is highly sensitive towards spatial conformations,[20] the comparison of ECD spectra, in particular with those of complexes that have been studied by X-ray crystallography, represents an efficient way to assign absolute configurations through the identification of invariant bands or bisignate patterns in a specific region. ECD spectra of 1st eluted complexes **9 b–e** are depicted in Figure 6. A similar shape was observed for complexes **9 c–e** with a negative ECD-active band between 195 and 200 nm, albeit differential molar extinctions (Δε) were slightly different. Due to the low ECD signal observed for **9 b**, its absolute configuration cannot be confidently deduced from the comparison with other ECD spectra.

As displayed in Figure 7, ECD spectra of first eluted chiral Pd(cinnanyl)Cl(NHC) complexes **10 e–g** were perfectly superposable with two negative ECD-active bands at 195 (Δε = −55; −78 for **10 g**) and 265 nm (Δε = −5) and one positive band at 225 nm (Δε = +10). This perfect match might be due to both N-aryl groups that restrict several rotations in complexes structures and thus provide a more rigid chiral environment. In the case, the absolute configuration of complexes **10 e** and **10 f** can be confidently assigned as (S_a)-(−) for the first eluted enantiomers.

The assignment of the absolute configuration of complex **10 e** was confirmed by the ECD spectra comparison between allyl- and cinnamyl complexes **9 e** and **10 e**, respectively (Figure 8). The perfect concordance between both spectra enabled to attribute unambiguously the same configuration to enantiomers with the same elution order. A (R_a)-(+) absolute configuration was attributed to the second eluted enantiomer **9 e** through single crystal X-ray diffraction studies.

However, ECD spectra of allyl- and cinnamyl complexes **9 d** and **10 d** display almost mirror image with one negative ECD-active band at 195 (Δε = −26) and two small positive bands at 220 and 235 nm (Δε = +2) for **9 d** whereas **10 d** exhibited two positive bands at 195 (Δε = +15) and 270 nm (Δε = +8) as well as two small negative bands at 220 and 235 nm (Δε = −4 and −2, respectively) (Figure 9). This suggests obviously an inversion of the enantiomeric elution order by cHPLC on the same chiral column and with the same mobile phase[21] as hypothesized during the examination of specific rotations.

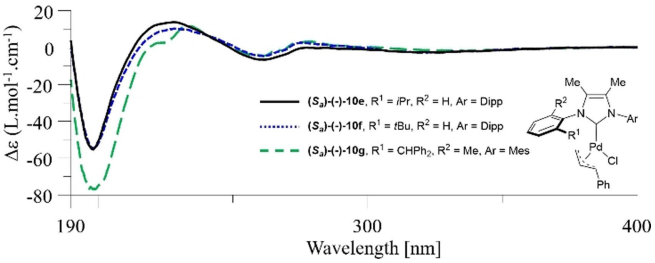

Figure 7. ECD spectra of first eluted complexes **10 e–g**.

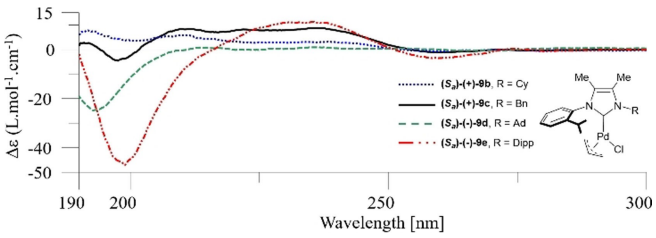

Figure 6. ECD spectra of first eluted complexes **9 b–e**.

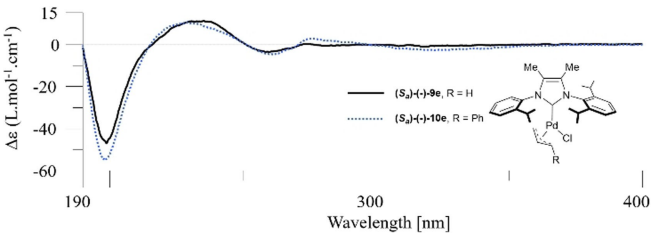

Figure 8. ECD spectra of first eluted complexes **9 e** and **10 e**.

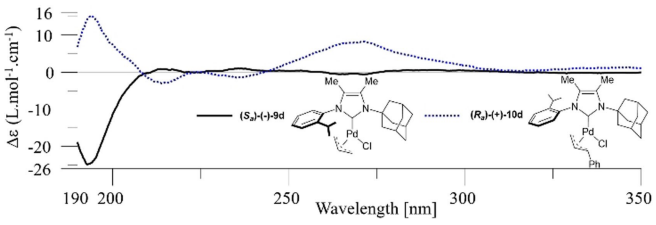

Figure 9. ECD spectra of first eluted complexes **9 d** and **10 d**.

Rotational Barriers Determination

The half-lifes of racemization for palladium complexes have been experimentally determined by following the decay of enantiomeric excesses over time at a given temperature and allowed to assess the values of rotational barriers (Figure 10).[17] Of note, the value of the rotational barrier for complex **10 b** could not be determined due to a rapid decomposition of the complex under the conditions to monitor the kinetic of enantiomerization (132 °C in chlorobenzene). Rotational barrier values for complex **10 f** containing a *tert*-butyl in *ortho* position and complexes **9 g** and **10 g** containing a benzhydryl moiety could not be measured. Thus, these complexes exhibit excellent conformation stability and degradation processes occurred before racemization (> 170 kJ.mol^{-1}, $t_{1/2}$ > 17 days at 180 °C). All the complexes containing an *iso*-propyl in *ortho* position displayed a rotation barrier value in range 131–139 kJ.mol^{-1}. This confirms the good conformational stability of these complexes: $t_{1/2}$ > 2 years at 50 °C or $t_{1/2}$ > 24 hours at 100 °C. As hypothesized, the nature of the second *N*-substituent (R) as a limited impact on the values of rotational barriers as well as the nature of the allyl ligand (allyl vs. cinnamyl). Theoretical calculations corroborated these findings, albeit the calculated values are slightly higher than the experimental values. For example, the lowest theoretically calculated value for structure **9 b** is 145.3 kJ.mol^{-1} vs. 138.5 kJ.mol^{-1} for the experimental value of complex **9 b**. Interestingly, theoretical calculations allowed to determine that the more favorable rotations take place on the palladium side ($\Delta G^{\neq}_{(Pd)}$).

In order to demonstrate that methyl groups on the NHC backbone were mandatory to restrict the rotation of *N*-aryl substituents along the C–N bond and thus obtain configurationnally stable chiral palladium-NHC complexes, complexes **11 b** and **12 b** possessing an unsubstituted saturated and unsaturated NHC backbone were prepared (Figure 11).[17] Unfortunately, no enantiomers could be detected by chiral HPLC analyses, even at low temperature. Rotational barriers for complexes **11 a** and **12 a** with a methyl as second *N*-

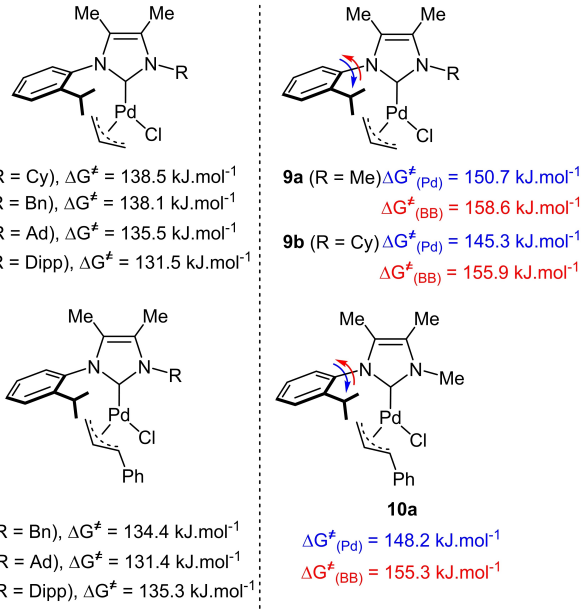

Figure 10. Values for the rotation barriers of Pd(NHC) complexes (left: experimentally determined; right DFT calculated).

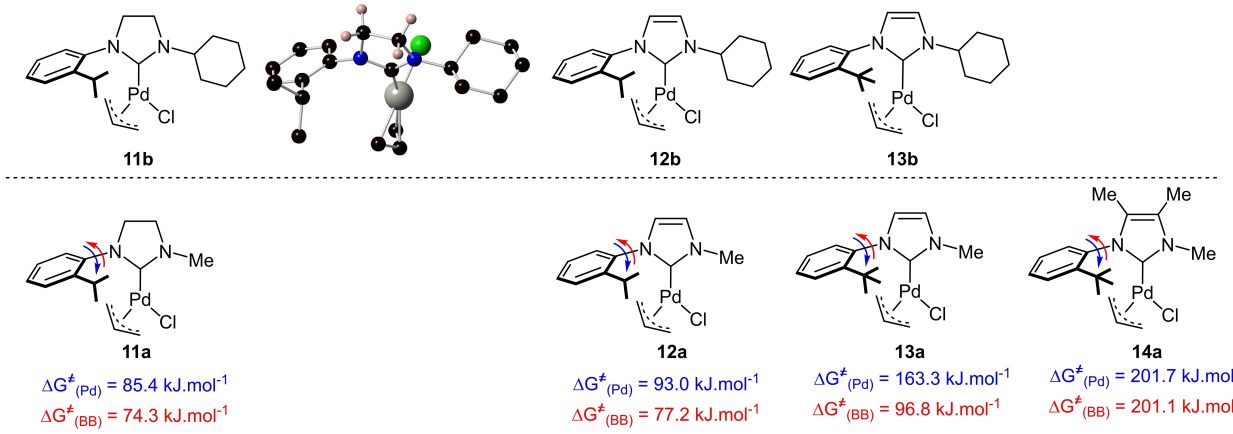

Figure 11. Influence of the backbone substitution on the rotation barriers.

substituent have been theoretically studied. The calculations show that rotations are more favorable on the backbone side with lower values by at least 10 kJ.mol^{-1}. The values of $\Delta G^{\neq}_{(BB)}$ were found close to 75 kJ.mol^{-1} (74.3 and 77.2 kJ.mol^{-1} for complexes **11 a** and **12 a**, respectively) which indicates half-lifes of racemization quicker than one second at 25 °C. As we were wondering if the replacement of the *iso*-propyl moiety by a more hindered *tert*-butyl could allow to significantly restricted the rotations with an unsubstituted backbone, calculations were performed for complex **13 a**. With $\Delta G^{\neq}_{(BB)} = 96.8$ kJ.mol^{-1}, it was expected to observe enantiomers and therefore complex **13 b** was synthesized.[17] Unfortunately, enantiomers of complex **13 b** could not be observed by cHPLC analyses suggesting that the value of the rotational barrier was slightly lower than 90 kJ.mol^{-1}. Of note, with a *tert*-butyl group and methyl substituents on the backbone, calculations gave rotational barrier values higher than 200 kJ.mol^{-1} (structure **14 a**).

Asymmetric Catalysis

The palladium-catalyzed intermolecular α-arylation of amide has been used as benchmark reaction to evaluate to ability of chiral palladium-based complexes, in particular containing chiral NHC ligands to induce efficiently an enantioselectivity.[4b,c,5d,9a,22] Therefore, we tested enantiopure complexes **9** and **10** in the intermolecular α-arylation of amide **15** (Scheme 6). Standard conditions reported in the literature, 1,2-dimethoxyethane (DME) at 60 °C in the presence of *t*-BuOK, were used, but only low enantiomeric excess

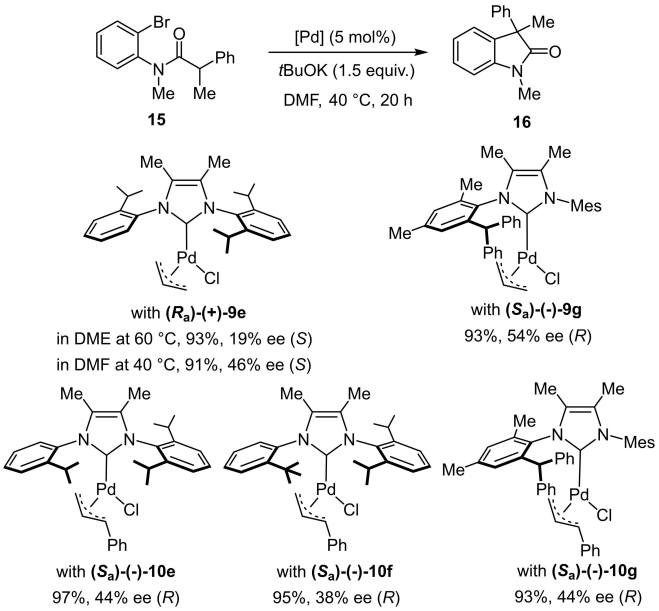

Scheme 6. Palladium-catalyzed Intermolecular α-arylation of amide **15**.

were obtained. For instance, complex **(R_a)-(+)-9 e** afforded the expected oxindole in good yield (93%) but with only 19% ee. When the same reaction was carried in DMF, reactivity was found higher and allowed to decrease the reaction temperature to 40 °C. Moreover, an improved enantioselectivity was observed: 46% ee. A similar chiral induction was obtained with the cinnamyl analogue **(S_a)-(−)-10 e**, 44% ee with 97% yield. Complex **(S_a)-(−)-10 f** containing a *tert*-butyl group instead of an i*so*-propyl gave a slightly lower enantioselectivity (38% ee). The best enantiomeric excess, 54%, was obtained with complex **(S_a)-(−)-9 g** whereas the cinnamyl analogue **(S_a)-(−)-10 g** gave 44% ee. These levels of chiral induction were significantly lower than those generally observed with C_2-symmetric chiral NHC ligands. This might be the result of an unrestricted rotation of the NHC along the carbene-metal bond.[22f]

Conclusion

In summary, we reported the synthesis of new class of chiral palladium complexes bearing C_1-symmetric NHC ligands. The chirality of theses complexes resulted from the metalation step which restricted the rotation of dissymmetric *N*-aryl substituents of NHCs and thus created an axis of chirality. Due to the excellent stability of these complexes, a resolution by chiral HPLC at preparative scale (up to 250 mg scale) allowed to obtain enantiopure complexes. Remarkably, all the palladium complexes could be separated by cHPLC with excellent enantiopurities (typically >99.5% ee). Analyses by X-ray crystallography of some complexes confirmed molecular structures and determined absolute configurations. ECD spectra were recorded for all complexes and allowed to deduce absolute configurations. Experimental and theoretical investigations of the rotational barriers highlighted that the metalation step enabled the formation of configurationally stable Pd–NHC complexes from imidazolium salts existing in solution as rotamers. Moreover, it has been demonstrated that the substitution the NHC backbone with methyl groups was a key parameter to prevent the rotation of *N*-aryl substituents on the backbone side. Finally, palladium complexes exhibited good catalytic activities in the intramolecular α-arylation of amides, albeit with moderate enantioselectivities. Nevertheless, enantiomeric excesses were found higher than those reached with analogous palladium complexes containing chiral C_1-symmetric NHC ligands.

Experimental Section

Preparation of Dissymmetrical Imidazolium Salts 4 – General Procedure A

To a suspension of formamidine (1 mmol) in acetonitrile (2 mL), *N,N*-Diisopropylethylamine (0.35 mL, 2 mmol, 2.0 equiv.) and 3-bromo-2-butanone (0.21 mL, 2 mmol, 2.0 equiv.) were added and the resulting mixture was stirred at 110 °C for 20 h. The solvent was removed under vacuum. The residue was purified by silica gel flash chromatography (petroleum ether/ethyl acetate = 10:1) to give the intermediate. The intermediate was dissolved in dichloromethane (3 mL). Triethylamine (142 µL, 1.1 mmol, 1.1 equiv.) was added dropwise at −40 °C. After 5 min, trifluoromethanesulfonic anhydride (188 µL, 1.1 mmol, 1.1 equiv.) was added dropwise. The mixture was slowly warmed up to room temperature and stirred at room temperature for 4 hours. The volatiles were removed under vacuum and the residue was purified by silica gel column (dichloromethane/acetone = 10:1) to give the imidazolium salt **4**.

Preparation of Dissymmetric Formamidines 6 – General Procedure B

Acetic acid (86 µL, 1.5 mmol, 0.05 equiv.) was added to a round bottom flask charged with the first amine (30 mmol, 1.0 equiv.) and triethyl orthoformate (5 mL, 30 mmol, 1.0 equiv.). The flask was fitted with a distillation head and was stirred and heated to 140 °C until ethanol (3.5 mL, 60 mmol, 2.0 equiv) was collected by distillation. The second amine (30 mmol, 1.0 equiv) was then added to the reaction mixture. Heating at 140 °C continued until ethanol (1.75 mL, 30 mmol, 1 equiv.) was collected by distillation. Workup was performed as indicated below, either by washing with cold (5–15 °C) *n*-hexane and then either recrystallization or flash chromatography.

Synthesis of the NHC-Palladium Complexes 9–13 – General Procedure C

A mixture of imidazolium tetrafluoroborate (or imidazolium trifluoromethylsufonate) (2.3 mmol, 2.3 equiv.), [Pd(cinnamyl)Cl]$_2$ or [Pd(allyl)Cl]$_2$ (1.0 mmol, 1.0 equiv.), KO*t*Bu (2.3 mmol, 2.3 equiv.) in acetone was stirred at 25 °C for 5 h. The reaction mixture was filtered through a Celite® pad and the solvent was removed under vacuum. The crude product was purified by silica gel column (PE/Et$_2$O = 1:1) give the expected NHC-palladium complex.

Crystallographic Data

CCDC numbers 1918272 (**(*R*$_a$)-(+)-9 e**), 2049183 (**(*R*$_a$)-(−)-9 c**), 2049184 (**(*R*$_a$)-(+)-9 g**), 2049185 (**(*R*$_a$)-(+)-10 g**) and 2049186 (**11 b**) contain the supplementary crystallographic data for this paper. These data can be obtained free of charge from The Cambridge Crystallographic Data Centre via www.ccdc.cam.ac.uk/data_request/cif.

Acknowledgements

We are grateful to the CNRS, Aix-Marseille Université and the ECM. L.K. and Y.C. thank the China Scholarship Council for Ph.D. grants. We acknowledge the Agence Nationale de la Recherche (ANR-20-CE07-0030 cResolu). We thank the Spectropole, Fédération des Sciences de Marseille, in particular Dr. Roseline Rosas for VT-NMR spectroscopy, Dr. Michel Giorgi for DRX and Dr. Valérie Monnier and Dr. Christophe Chendo for HRMS as well as Arnaud Treuvey (ECM) for IR spectroscopy. Umicore AG & Co is acknowledged for a generous gift of complexes.

References

[1] a) S. P. Nolan (Ed.), *N-Heterocyclic Carbenes Effective Tools for Organometallic Synthesis*; Wiley-VCH: Weinheim **2014**; b) S. Díez-González (Ed.), *N-Heterocyclic Carbenes: From Laboratory Curiosities to Efficient Synthetic Tools: Edition 2*; The Royal Society of Chemistry: Cambridge, U. K. **2017**; c) H. V. Huynh, *The Organometallic Chemistry of N-heterocyclic Carbenes; Inorganic Chemistry: A Textbook Series*, Wiley, Hoboken **2017**.

[2] S. Díez-Gonzalez, N. Marion, S. P. Nolan, *Chem. Rev.* **2009**, *109*, 3612–3676.

[3] a) F. Wang, L.-J. Liu, W. Wang, S. Li, M. Shi, *Coord. Chem. Rev.* **2012**, *256*, 804–853; b) D. Janssen-Müller, C. Schlepphorst, F. Glorius, *Chem. Soc. Rev.* **2017**, *46*, 4845–4854; c) P. J. Czerwiński, M. Michalak, *Synthesis* **2019**, *51*, 1689–1714.

[4] For representative examples, see: a) W. A. Herrmann, L. J. Goossen, G. R. Artus, C. Köcher, *Organometallics* **1997**, *16*, 2472–2477; b) S. Lee, J. F. Hartwig, *J. Org. Chem.* **2001**, *66*, 3402–3415; c) E. P. Kündig, T. M. Seidel, Y.-x. Jia, G. Bernardinelli, *Angew. Chem. Int. Ed.* **2007**, *46*, 8484–8487; *Angew. Chem.* **2007**, *119*, 8636–8639; d) S. Urban, N. Ortega, F. Glorius, *Angew. Chem. Int. Ed.* **2011**, *50*, 3803–3806; *Angew. Chem.* **2011**, *123*, 3887–3890; e) A. Albright, D. Eddings, R. Black, C. J. Welch, N. N. Gerasimchuk, R. E. Gawley, *J. Org. Chem.* **2011**, *76*, 7341–7351; f) A. Albright, R. E. Gawley, *J. Am. Chem. Soc.* **2011**, *133*, 19680–19683; g) D. Shen, Y. Xu, S.-L. Shi, *J. Am. Chem. Soc.* **2019**, *141*, 14938–14945; h) Z.-C. Wang, P.-P. Xie, Y. Xu, X. Hong, S.-L. Shi, *Angew. Chem. Int. Ed.* **2021**, doi.org/10.1002/anie.202103803; *Angew. Chem.* **2021**, doi.org/10.1002/ange.202103803.

[5] For selected publications, see: a) S. Würtz, C. Lohre, R. Fröhlich, K. Bergander, F. Glorius, *J. Am. Chem. Soc.* **2009**, *131*, 8344–8345; b) D. Baskakov, W. A. Herrmann, E. Herdtweck, S. D. Hoffmann, *Organometallics* **2007**, *26*, 626–632; c) C. Metallinos, X. Du, *Organometallics* **2009**, *28*, 1233–1242; d) C. Xu, Y. Feng, L.-R. Wang, W.-P. Ma, Y.-M. He, Q.-H. Fan, *Organometallics* **2020**, *39*, 1945–1960.

[6] For selected publications, see: a) D. R. Jensen, M. S. Sigman, *Org. Lett.* **2003**, *5*, 63–65; b) J. Pytkowicz, R.

Roland, P. Mangeney, G. Meyer, A. Jutand, *J. Organomet. Chem.* **2003**, *678*, 166–179; c) T. Arao, K. Kondo, T. Aoyama, *Tetrahedron Lett.* **2006**, *47*, 1417–1420; d) K. B. Selim, Y. Matsumoto, K.-i. Yamada, K. Tomioka, *Angew. Chem. Int. Ed.* **2009**, *48*, 8733–8735; *Angew. Chem.* **2009**, *121*, 8889–8891; e) H. Wang, G. Lu, G. J. Sormunen, A. Hasnain, H. A. Malik, P. Liu, J. Montgomery, *J. Am. Chem. Soc.* **2017**, *139*, 9317–9324; f) W.-Y. Wang, J.-Y. Wu, Q.-R. Liu, X.-Y. Liu, C.-H. Ding, X.-L. Hou, *Org. Lett.* **2018**, *20*, 4773–4776; g) Y. Chen, L. Dang, C.-Y. Ho, *Nat. Commun.* **2020**, *11*, 2269.

[7] T. J. Seiders, D. W. Ward, R. H. Grubbs, *Org. Lett.* **2001**, *3*, 3225–3228.

[8] For representative examples, see: a) M. R. Chaulagain, G. J. Sormunen, J. Montgomery, *J. Am. Chem. Soc.* **2007**, *129*, 9568–9569; b) C.-Y. Ho, C.-W. Chan, L. He, *Angew. Chem. Int. Ed.* **2015**, *54*, 4512–4516; *Angew. Chem.* **2015**, *127*, 4595–4599; c) R. Kumar, Y. Hoshimoto, H. Yabuki, M. Ohashi, S. Ogoshi, *J. Am. Chem. Soc.* **2015**, *137*, 11838–11845; d) J. S. E. Ahlin, N. Cramer, *Org. Lett.* **2016**, *18*, 3242–3245; e) Z. Li, L. Zhang, M. Nishiura, G. Luo, Y. Luo, Z. Hou, *ACS Catal.* **2020**, *10*, 11685–11692.

[9] a) X. Luan, R. Mariz, C. Robert, M. Gatti, S. Blumentritt, A. Linden, R. Dorta, *Org. Lett.* **2008**, *10*, 5569–5572; b) X. Luan, R. Mariz, M. Gatti, C. Costabile, A. Poater, L. Cavallo, A. Linden, R. Dorta, *J. Am. Chem. Soc.* **2008**, *130*, 6848–6858.

[10] a) D. S. Clyne, J. Jin, E. Genest, J. C. Gallucci, T. V. Rajanbabu, *Org. Lett.* **2000**, *2*, 1125–1128; b) W. L. Duan, M. Shi, G.-B. Rong, *Chem. Commun.* **2003**, 2916–2917; c) L.-j. Liu, F. Wang, M. Shi, *Organometallics* **2009**, *28*, 4416–4420; d) C. Bartolomé D García-Cuadrado, Z. Ramiro, P. Espinet, *Inorg. Chem.* **2010**, *49*, 9758–9764; e) Y.-M. Wang, C. N. Kuzniewski, V. Rauniyar, C. Hoong, F. D. Toste, *J. Am. Chem. Soc.* **2011**, *133*, 12972–12975.

[11] a) J. J. Van Veldhuizen, S. B. Garber, J. S. Kingsbury, A. H. Hoveyda, *J. Am. Chem. Soc.* **2002**, *124*, 4954–4955; b) S. Handa, L. M. Slaughter, *Angew. Chem. Int. Ed.* **2012**, *51*, 2912–2915; *Angew. Chem.* **2012**, *124*, 2966–2969.

[12] a) J. Francos, F. Grande-Carmona, H. Faustino, J. Iglesias-Sigüenza, E. Díez, I. Alonso, R. Fernández, J. M. Lassaletta, F. López, J. L. Mascareñas, *J. Am. Chem. Soc.* **2012**, *134*, 14322–14325; b) F. Grande-Carmona, J. Iglesias-Sigüenza, E. Álvarez, E. Díez, R. Fernández, J. M. Lassaletta, *Organometallics* **2015**, *34*, 5073–5080; c) I. Varela, H. Faustino, E. Díez, J. Iglesias-Sigüenza, J. Grande-Carmona, F. Fernández, R. Lassaletta, J. M. Mascareñas, J. L. López, *ACS Catal.* **2017**, *7*, 2397–2402.

[13] L. Kong, J. Morvan, D. Pichon, M. Jean, M. Albalat, T. Vives, S. Colombel-Rouen, M. Giorgi, V. Dorcet, T. Roisnel, C. Crévisy, D. Nuel, P. Nava, S. Humbel, N. Vanthuyne, M. Mauduit, H. Clavier, *J. Am. Chem. Soc.* **2020**, *142*, 93–98.

[14] A. Fürstner, M. Alcarazo, V. César, C. W. Lehmann, *Chem. Commun.* **2006**, 2176–2178.

[15] K. Hirano, S. Urban, C. Wang, F. Glorius, *Org. Lett.* **2009**, *11*, 1019–1022.

[16] J. Zhang, J. Fu, X. Su, X. Wang, S. Song, M. Shi, *Chem. Asian J.* **2013**, *8*, 552–555.

[17] For details, see supporting information.

[18] N. Marion, O. Navarro, J. Mei, E. D. Stevens, N. M. Scott, S. P. Nolan, *J. Am. Chem. Soc.* **2006**, *128*, 4101–4111.

[19] L. Falivene, Z. Cao, A. Petta, L. Serra, A. Poater, R. Oliva, V. Scarano, L. Cavallo, *Nat. Chem.* **2019**, *11*, 872–879.

[20] G. Pescitelli, L. Di Bari, N. Berova, *Chem. Soc. Rev.* **2011**, *40*, 4603–4625.

[21] N. Vanthuyne, C. Roussel, *Chiroptical Detectors for the Study of Unusual Phenomena in Chiral Chromatography; In Differentiation of Enantiomers I. Topics in Current Chemistry*, V. Schurig (Ed.), Springer, Cham., **2013**, vol. 340, pp. 107–151.

[22] For selected examples, see: a) Y.-X. Jia, J. M. Hillgren, E. L. Watson, S. P. Marsden, E. P. Kündig, *Chem. Commun.* **2008**, 4040–4042; b) S. Würtz, C. Lohre, R. Fröhlich, K. Bergander, F. Glorius, *J. Am. Chem. Soc.* **2009**, *131*, 8344–8345; c) X. Luan, L. Wu, E. Drinkel, R. Mariz, M. Gatti, R. Dorta, *Org. Lett.* **2010**, *12*, 1912–1915; d) L. Liu, N. Ishida, S. Ashida, M. Murakami, *Org. Lett.* **2011**, *13*, 1666–1669; e) L. Wu, L. Falivene, E. Drinkel, S. Grant, A. Linden, L. Cavallo, R. Dorta, *Angew. Chem. Int. Ed.* **2012**, *51*, 2870–2873; *Angew. Chem.* **2012**, *124*, 2924–2927; f) D. Katayev, Y.-X. Jia, A. K. Sharma, D. Banerjee, C. Besnard, R. B. Sunoj, E. P. Kündig, *Chem. Eur. J.* **2013**, *19*, 11916–11927.

